Approximating the kinematics of converted waves

Chuck Sword

INTRODUCTION

Converted-wave reflections are usually difficult to process, because they exhibit non-regular travel-time curves (i.e., non-regular kinematics). For instance, on a common-midpoint (CMP) gather the travel-time curve of a converted wave, unlike that of a simple PP or SS wave, is non-symmetrical if the reflector is slanted. The processing difficulties caused by this effect should be obvious. In this paper I will present a simple transformation of the coordinates of converted-wave data. This transformation is partially based on work by Nefedkina (1980), and by Puzyrev (1975), who are studying similar problems in Novosibirsk. If the coordinates of the data are thus transformed, they will appear to have (approximately) the kinematics of normal PP or SS data, and can subsequently be processed using already-existing techniques (e.g., velocity analysis, dip moveout (DMO) (Hale, 1983), NMO and stack, migration, even controlled directional reception (CDR) (Sword, 1984)). The individual data traces are not altered by the transformation; they are merely given new coordinates (that is, new midpoints and offsets), based on an a priori knowledge of the ratio v_P/v_S.

I will show that as long as the ratio v_P/v_S is constant over the entire section, and v_P is a function of z (depth) only, the kinematics of the transformed data will approximate the kinematics of normal PP or SS data. I will also present graphs that indicate the accuracy of the approximation under various conditions, and I will compare synthetic converted-wave data processed with these techniques to the same data processed with conventional techniques. In the Appendix I will show how I originally derived the transformation; in the body of the paper I will only present the transformation and show how it works.

NOTATION

It is useful to begin by establishing a consistent system of notation. Figure 1 shows a typical recording geometry.

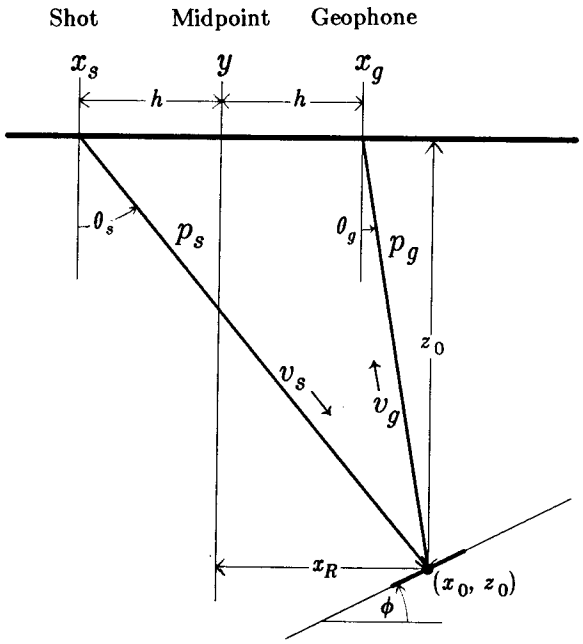

FIG. 1. Typical recording geometry. The figure is drawn so that all parameters shown on it are positive.

The notation used in this paper is:

x_s	–	Shot position
x_g	–	Geophone position
h	–	Half-offset: $(x_g - x_s)/2$
y	–	Midpoint: $(x_s + x_g)/2$
x_0, z_0	–	Reflector position
x_R	–	Horizontal distance from the midpoint y to the reflector
t	–	Travel time
v_s	–	Velocity from shot to reflector (velocity of the downgoing ray)
v_g	–	Velocity from reflector to geophone (velocity of the upcoming ray)
γ	–	Ratio of velocities: v_g / v_s
p_s	–	Ray parameter of the downgoing ray ($p_s = -dt/dx_s$)
p_g	–	Ray parameter of the upcoming ray ($p_g = -dt/dx_g$)

This notation can be a bit misleading at first. For example, if we were interested in PS waves, v_s would be the P-wave velocity, while v_g would be the S-wave velocity. In other words, it is wrong to always assume that v_s equals the S-wave velocity v_S. It should be noted that for PP or SS waves $\gamma = 1$, while for PS waves $\gamma < 1$, and for SP

waves $\gamma > 1$.

THE TRANSFORMATION

The transformation is very simple. If we have a trace that was recorded at midpoint y and offset h, we simply give it new coordinates y' and h', where

$$y' \equiv y - h \cdot \frac{1 - \frac{1}{\gamma}}{1 + \frac{1}{\gamma}} \tag{1}$$

and

$$h' \equiv h \cdot \frac{2}{\sqrt{\gamma}\left(1 + \frac{1}{\gamma}\right)}. \tag{2}$$

We also define a new velocity v, where

$$v \equiv \frac{2 v_s}{1 + \frac{1}{\gamma}}. \tag{3}$$

This last definition is not a transformation of the data, but we will see (in the following section) that this definition is useful when the transformed data is being processed and interpreted. (The derivation of these three equations is given in the Appendix.) Equation (1), by the way, was originally developed and tested by researchers at the Institute of Geology and Geophysics in Novosibirsk (see Nefedkina, 1980; Nefedkina, et al., 1980; and Puzyrev, 1975); they made no transformation analogous to equation (2), and defined their velocity transform as $v \equiv \sqrt{v_s\, v_g}$. Their transforms make it possible to perform NMO on, and to stack, converted-wave data in a reasonable way, but the velocity v cannot be directly used for the subsequent migration, and it is not entirely clear how more complex pre-stack operations, such as DMO, can be accommodated.

We will see in the following section that after the transformations given in equations (1), (2), and (3) are performed, the transformed converted-wave kinematics will approximate the kinematics of untransformed PP or SS data. It is useful, however, as a preliminary step, to see what other transformations are produced as a consequence of those given above. Combining the definitions in the "Notation" section with equations (1) and (2), we find that

$$x_s' = \frac{1}{\sqrt{\gamma}\left(1 + \frac{1}{\gamma}\right)} \left[\left(\sqrt{\gamma} + 1\right) x_s + \left(\frac{1}{\sqrt{\gamma}} - 1\right) x_g \right] \tag{4a}$$

and

$$x_g' = \frac{1}{\sqrt{\gamma}\left(1+\frac{1}{\gamma}\right)}\left[\left(\sqrt{\gamma}-1\right)x_s + \left(\frac{1}{\sqrt{\gamma}}+1\right)x_g\right]. \tag{4b}$$

Then we recall that $p_s = -dt/dx_s$, $p_s' = -dt/dx_s'$, etc.; by using the chain rule to expand these definitions, and by making use of equations (4a) and (4b), we find that

$$p_s' = \frac{1}{2}\left[\left(1+\frac{1}{\sqrt{\gamma}}\right)p_s + \left(1-\sqrt{\gamma}\right)p_g\right] \tag{5a}$$

and

$$p_g' = \frac{1}{2}\left[\left(1-\frac{1}{\sqrt{\gamma}}\right)p_s + \left(1+\sqrt{\gamma}\right)p_g\right]. \tag{5b}$$

These two equations will be useful in the proof that follows; they are also useful when one is processing data using the method of Controlled Directional Reception (Sword, 1984).

APPROXIMATING THE TRAVEL TIME

If we have a layered medium (that is, $v = v(z)$), then according the laws of ray tracing we can write

$$t = \int_0^z \frac{dz}{v_s(z)\sqrt{1-p_s^2 v_s^2(z)}} + \int_0^z \frac{dz}{v_g(z)\sqrt{1-p_g^2 v_g^2(z)}}. \tag{6}$$

Differentiating with respect to z, we can then state that for all z (at least, for all z such that z is less than the reflector's depth)

$$\frac{dt}{dz} = \frac{1}{v_s\sqrt{1-p_s^2 v_s^2}} + \frac{1}{v_g\sqrt{1-p_g^2 v_g^2}}. \tag{7}$$

Recall that from our original definitions, $v_g(z) = \gamma v_s(z)$, with γ constant, so that

$$\frac{dt}{dz} = \frac{1}{v_s\sqrt{1-p_s^2 v_s^2}} + \frac{1}{\gamma v_s\sqrt{1-\gamma^2 p_g^2 v_s^2}}. \tag{8}$$

My claim is that after converted-wave data is transformed into the new system of coordinates outlined in the previous section, then the kinematics of these converted-wave events will approximate the kinematics of conventional waves in the regular system of coordinates. Equation (8) is a step in this proof: it represents the kinematics of converted waves in a medium in which v is a function of z. When $\gamma = 1$, equation (8) also represents the kinematics of conventional waves.

We can approximate equation (8) by means of a truncated Taylor series expansion:

$$\frac{1}{\sqrt{1-x}} \approx 1 + \frac{1}{2}x\,, \tag{9}$$

which gives us

$$\frac{dt}{dz} \approx \frac{1}{v_s} + \frac{1}{2}{p_s}^2 v_s + \frac{1}{\gamma v_s}\frac{1}{2\gamma}\gamma^2 {p_g}^2 v_s\ . \tag{10}$$

We can now rewrite equations (5) so that

$$p_s = \frac{1}{\sqrt{\gamma}\left(1+\frac{1}{\gamma}\right)}\left[\left(\sqrt{\gamma}+1\right)p_s' + \left(\sqrt{\gamma}-1\right)p_g'\right] \tag{11a}$$

and

$$p_g = \frac{1}{\sqrt{\gamma}\left(1+\frac{1}{\gamma}\right)}\left[\left(\frac{1}{\sqrt{\gamma}}-1\right)p_s' + \left(\frac{1}{\sqrt{\gamma}}+1\right)p_g'\right]. \tag{11b}$$

Substituting these, and equation (3), into equation (10), and doing a bit of algebra, we obtain

$$\frac{dt}{dz} \approx \frac{2}{v} + \frac{1}{2}v\left({p_s'}^2 + {p_g'}^2\right). \tag{12}$$

(The approximation sign ($\approx$) is from equation (10). No further approximations have been made.)

So now we have an expression that shows, approximately, how converted waves behave in the transformed coordinate system. The question is, does this expression matches the approximate kinematics of conventional waves in the untransformed coordinate system? By making the substitutions $\gamma = 1$ and $v = v_s$ into equation (8), and once again making the approximation shown in equation (9), we obtain the approximate kinematics for conventional waves:

$$\frac{dt}{dz} \approx \frac{2}{v} + \frac{1}{2}v\left({p_s}^2 + {p_g}^2\right). \tag{13}$$

Equations (12) and (13) match, so my claim is justified: By means of the transformations outlined in equations (1), (2), and (3), converted-wave data can take on the approximate kinematics of conventional data, and thus can be processed by existing methods.

HOW GOOD IS THE APPROXIMATION?

It is reasonable to wonder about the accuracy of the approximation described in the previous sections. In other words, after the transformation, how closely do the kinematics of the converted-wave data mimic those of conventional data? In this section are shown the results of some numerical tests.

One convenient way of displaying travel-time curves is in the form of a contoured surface in which the horizontal coordinates are y and h or y' and h' (midpoint and half-offset, in the untransformed or transformed coordinate systems, respectively). These coordinates differ, of course, from the ray-parameter coordinates (p_s, p_g, p_s', p_g') that we have been using. The vertical (contoured) coordinate is the travel time of a ray traveling from a shot on the Earth's surface to a diffracting point located at $y = 0$, $z = z_0$, and back up to a geophone on the surface. If we assume that v_s is constant, the equation for this travel-time surface is

$$t = \frac{1}{v_s}\sqrt{(y-h)^2 + z_0^2} + \frac{1}{\gamma v_s}\sqrt{(y+h)^2 + z_0^2} \quad . \tag{14}$$

In Figure 2 is such a contoured surface for the case $\gamma = .5$, $v_s = 3$ km/sec, and $z_0 = 1$ km, with a contour interval of .01 sec. The horizontal coordinates are y and h.

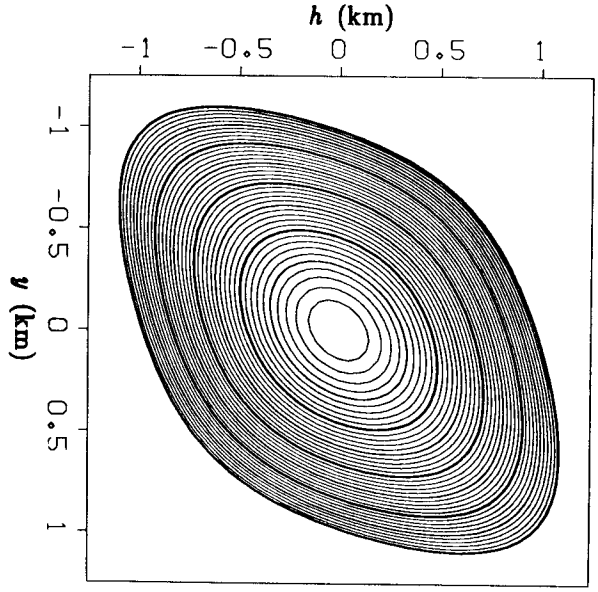

FIG. 2. A contoured converted-wave travel-time surface based on equation (14), in the original system of coordinates (y, h). For this figure, $\gamma = .5$, $v_s = 3$ km/sec, and $z_0 = 1$ km. The contour interval is .01 sec.

In Figure 3 is shown the same contoured surface, except that the horizontal coordinates are now y' and h'. This change of coordinates can be accomplished by rewriting equations (1) and (2) in the form

$$h = h'\frac{\sqrt{\gamma}}{2}\left(1 + \frac{1}{\gamma}\right) , \tag{15}$$

$$y = y' + h'\frac{\sqrt{\gamma}}{2}\left(1 - \frac{1}{\gamma}\right) , \tag{16}$$

and then substituting equations (15) and (16) in equation (14), the travel-time equation. The velocity can be transformed from v_s to v by means of equation (3).

So far we have made no approximations. Figure 3 shows the exact travel-time curve of a converted wave in the new system of coordinates. In Figure 4, however, is shown the travel-time curve that I have claimed to be approximately the same as that shown in Figure 3. That is, Figure 4 shows the travel-time curve of an unconverted wave, but one whose defining equation is given in transformed coordinates:

$$t = \frac{1}{v}\sqrt{(y'-h')^2+z_0^2} + \frac{1}{v}\sqrt{(y'+h')^2+z_0^2} \quad . \tag{17}$$

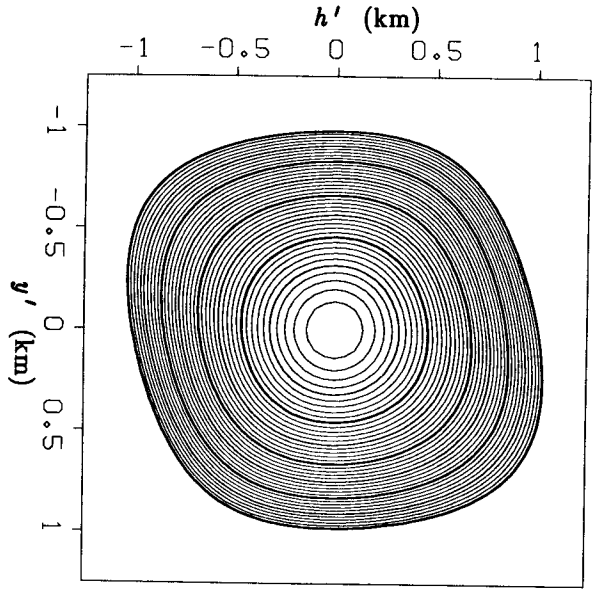

FIG. 3. Another contoured converted-wave travel-time surface based on equation (14), but this time in the new coordinate system y', h'. All other parameters, including the contour interval of .01 second, are the same as those in Figure 2.

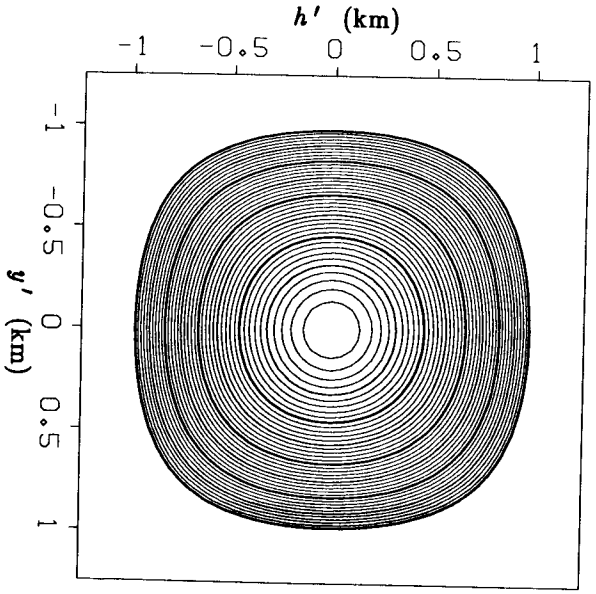

FIG. 4. A contoured travel-time surface, this time based on equation (17). It shows the curve that Figure 3 should be approximating if the transformations in equations (1), (2), and (3) indeed make converted-wave data behave (kinematically) as ordinary PP or SS data. All parameters are the same as those in Figures 2 and 3.

This equation reflects my claim that the converted-wave travel-time curves in the new coordinate system are similar to conventional curves in the old system.

The important issue, of course, is how well the two curves, the one in Figure 3 and the one in Figure 4, match. The answer is shown in Figure 5. Here we see the percentage error, given according to the formula $error \equiv (t_{FIG\,3} - t_{FIG\,4})/t_0$. Here $t_{FIG\,3}$ and $t_{FIG\,4}$ are the travel times shown in Figures 3 and 4, while t_0 is the travel time at the point $y = 0$, $h = 0$. The contour interval in this plot is 0.1% (0.001 in the above formula). Notice the new horizontal axes: y'/z_0 and h'/z_0. Thanks to the relative nature of the formula we are using, this plot will be unchanged for all values of z_0 and v_s (different values of γ will produce different plots, however).

This is an interesting plot, but it is plotted in a set of coordinates without an easily-visualized physical basis. To remedy this problem, Figure 6 shows the same results as Figure 5, but transformed back to the old coordinate system. Now the axes, y/z_0 and h/z_0, correspond to positions on the ground, and we can draw some conclusions about the accuracy of the approximation.

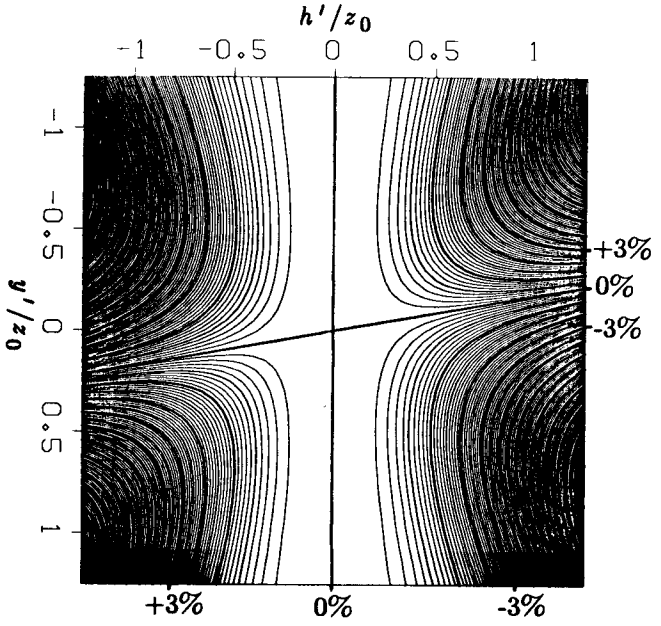

FIG. 5. Contour plot, in the transformed coordinate system, showing the percentage of error between the travel times in Figures 3 and 4. Note the z_0 term in the denominators of the two axes. As explained in the text, in this plot the only significant parameters are γ, which is 0.5, and the contour interval, which is 0.1%.

The first conclusion, which is immediately obvious, is that the approximation is best at zero offset (as will be shown in the Appendix, this conclusion isn't very surprising, because the transformation equations (1), (2), and (3) were derived so as to give that result). Next, it is apparent that the approximation has an error of less than 1% out to a half-offset h equal to $z_0/2$, where z_0 is the depth of the diffracting point reflector. (Keep in mind that if the half-offset is $z_0/2$, the actual distance from shot to receiver is z_0.) For half-offsets up to z_0 (and corresponding shot-receiver distances of up to $2z_0$),

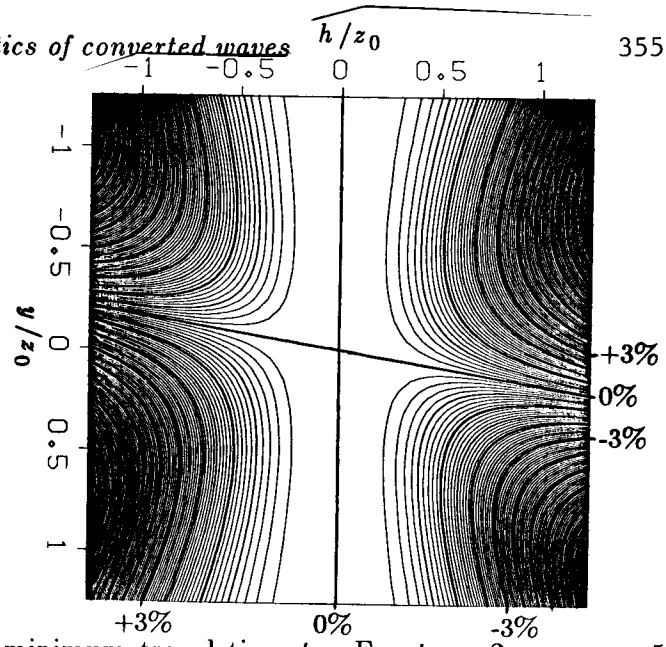

FIG. 6. Contour plot of the same error as that in Figure 5, but in the old system of coordinates. As in Figure 5, the only significant parameters are $\gamma = 0.5$ and the contour interval of 0.1%.

the error does not exceed 6% of the minimum travel time t_0. For $t_0 = 2$ sec, $\gamma = .5$, and a P-wave velocity of 3600 m/sec, this result implies that the error will be .02 sec when the distance from shot to geophone is 2400 m, and .12 sec when the shot-geophone distance is 4800 m.

DEALING WITH DATA: INTERPOLATION

One problem in implementing this transformation scheme is the necessity of interpolating data if conventional processing methods are to be used. For example, Figure 7 shows a typical stacking chart for conventionally-recorded data. Notice that the traces can easily be "binned" into common-midpoint gathers. In Figure 8 is the same stacking chart, after it has been transformed into the new coordinate system given by equations (1) and (2). The traces are no longer aligned along lines of common midpoint; thus it is no longer clear how such processes as CDP stacking should be carried out.

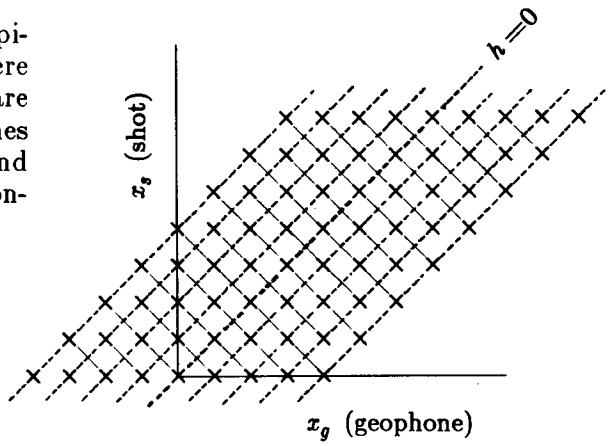

FIG. 7. Stacking chart for typical land seismic data, where $\Delta x_s = \Delta x_g$. Trace positions are indicated by x's. Dashed lines show common-offset gathers, and dotted lines show common-midpoint gathers.

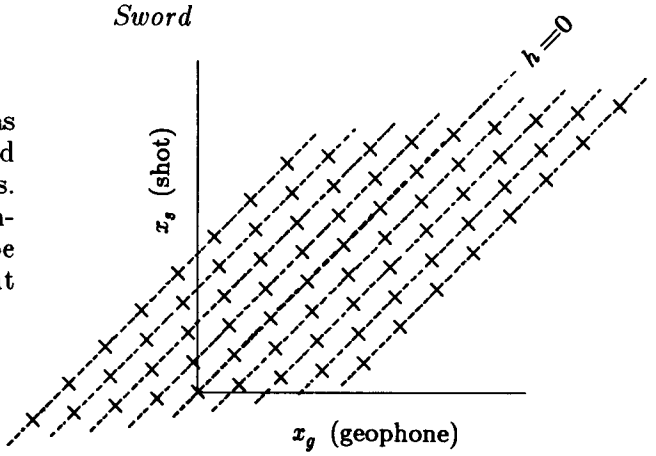

FIG. 8. Same stacking chart as that in Figure 7, but transformed to the new system of coordinates. Notice that common-offset gathers (dashed lines) can still be made, but that common-midpoint gathers can no longer be made.

The solution to this difficulty, of course, is some sort of interpolation. I chose to use nearest-neighbor interpolation along lines of common offset, as shown in Figure 9. If neither neighbor was considered "near" enough, no interpolated trace was generated. In tests with my relatively coarsely-sampled model data, the results of linear interpolation along common-offset lines were no better than those of the significantly-cheaper nearest-neighbor interpolation. The reason for interpolating along only common offsets rather than along both midpoint and offset axes is that by keeping offsets fixed, we don't risk destroying the relationship between travel-time and offset; this relationship is used in velocity analysis.

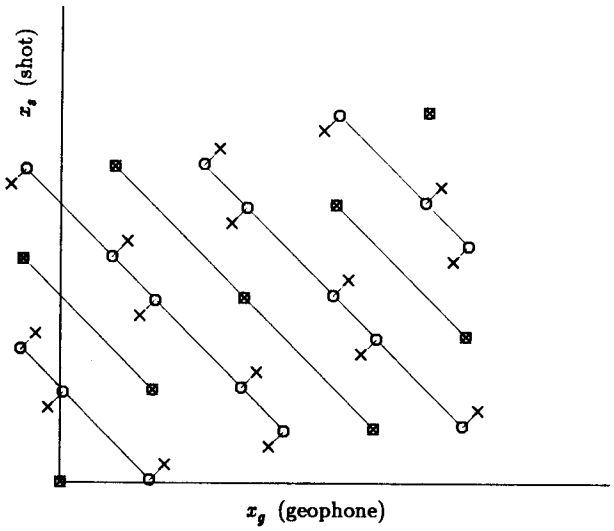

FIG. 9. Magnified portion of the transformed stacking chart in Figure 8. This shows the nearest-neighbor interpolation scheme. Interpolated traces are denoted by o's, which are connected to their nearest neighbors (x's) by short lines. Longer lines connect common-midpoint gathers.

COMPARISON OF SYNTHETIC DATA EXAMPLES

While I was in the Soviet Union I was given a synthetic converted-wave data set by Dr. G. Matveenko of VNII Geofizika. This data set was based on the model shown in Figure 10, which was developed by Boris Zavalishin of the Gubkin Institute in Moscow. The source produced both P-waves and S-waves, and the geophones were assumed to be vertical, so the predominant converted waves were of the SP type. The ratio γ was set

to be 1.732. The distances between geophones and between shots were both 100 meters, there were 51 shots with 25 geophones per shot, and the geophones were laid out in a symmetrical split-spread arrangement with one geophone lying directly on top of the shot (an advantage of synthetic data). As seen in Figure 10, the P-wave velocity (v_g in the SP-wave case) varied from 2300 to 4500 meters per second.

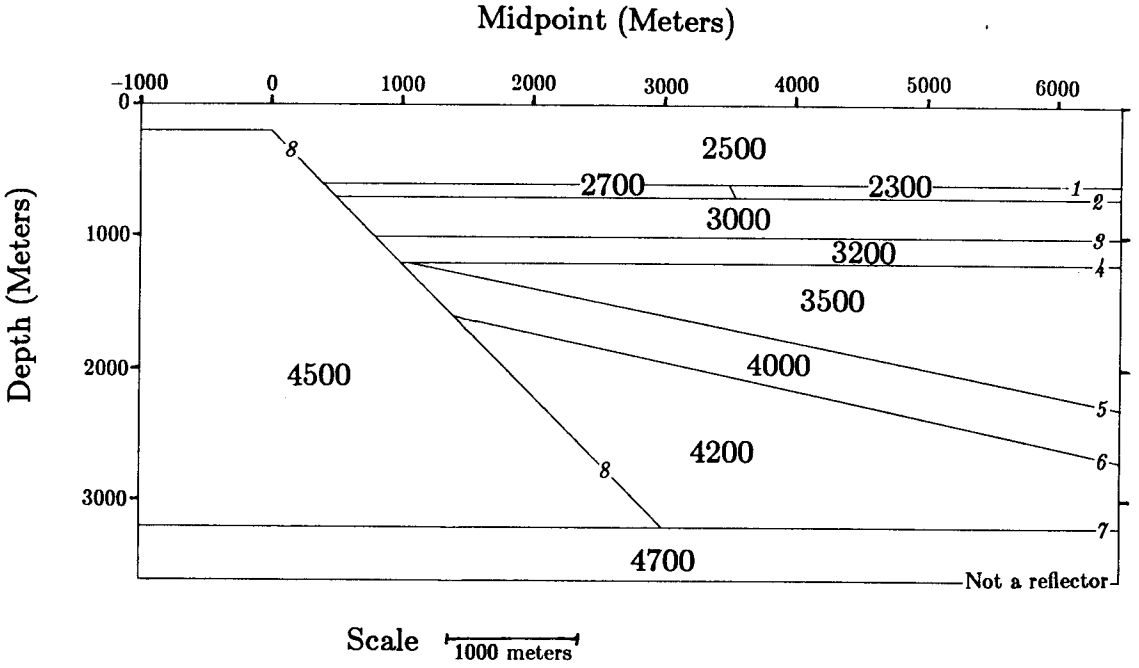

FIG. 10. Model used to generate the synthetic data in the subsequent figures. P-wave velocity (v_P) is shown in m/sec; S-wave velocity (v_S) is always $v_P/1.732$. Each reflector is labelled with a number. The source produces S- and P-waves of equal intensity, and the receivers are vertical geophones. Distances between shots and between geophones are each 100 m. No vertical exaggeration has been applied.

To show how the transformation affected processing, I processed this synthetic data both before and after making the transformations given in equations (1), (2), and (3). The first step in the processing involved performing velocity analyses every 500 meters. Figure 11 shows a velocity analysis, made on untransformed data, at $y = 3000$ m (this y is the horizontal axis in Figure 10). On it I have picked both PP and SP events. One interesting phenomenon is that the peaks corresponding to the SP-wave reflections from reflectors 5 and 6 (the gently-tilting reflectors in Figure 10) are split. This is the sort of behavior that makes processing converted-wave data difficult.

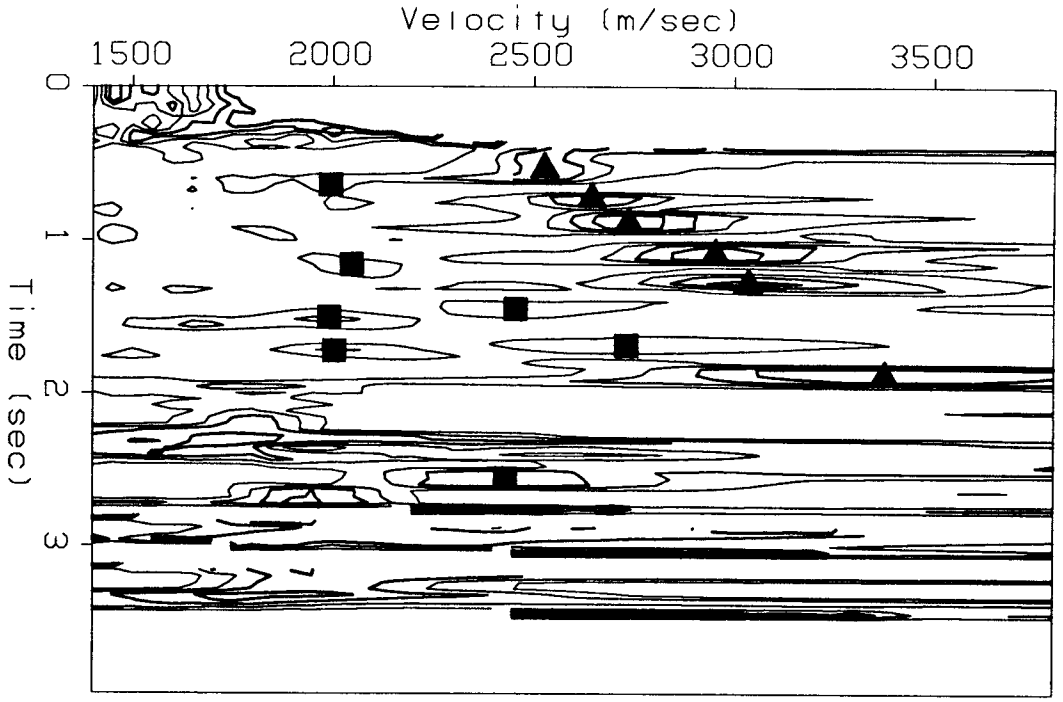

FIG. 11. Velocity analysis of an untransformed CMP gather, at midpoint $y = 3000$ m. Triangles denote P-wave velocity picks; squares denote converted-wave picks. Note the splitting on the converted-wave picks from reflectors 5 and 6.

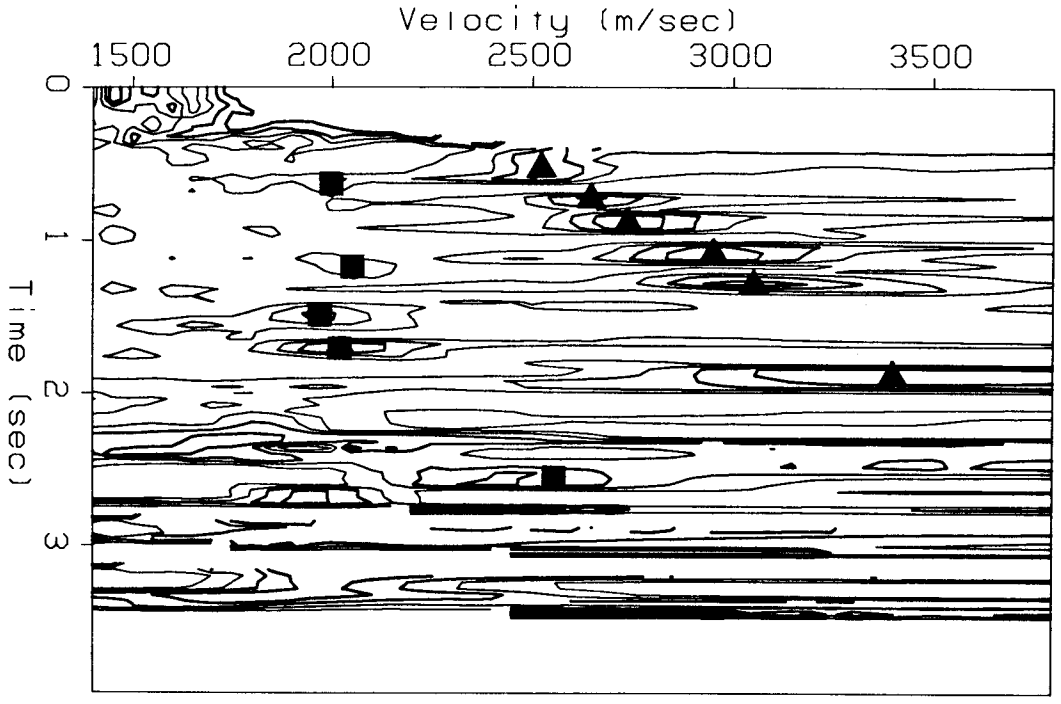

FIG. 12. Another velocity analysis of an untransformed CMP gather, also at midpoint $y = 3000$ m, but this time, only the up-dip half of the gather has been used. Again, triangles denote P-wave velocity picks and squares denote converted-wave picks. The splitting seen in Figure 11 is no longer evident.

Figure 12 is also a velocity analysis of untransformed data, and is also taken at the midpoint $y = 3000$ m, but this time the data set has been windowed so that only "up-dip" data (that is, data from geophones up-dip from the shot), remains. In this data set, which comes from a model whose dips are all in one direction, the term "up-dip" is unambiguous. Here the splitting noted in Figure 11 is no longer apparent.

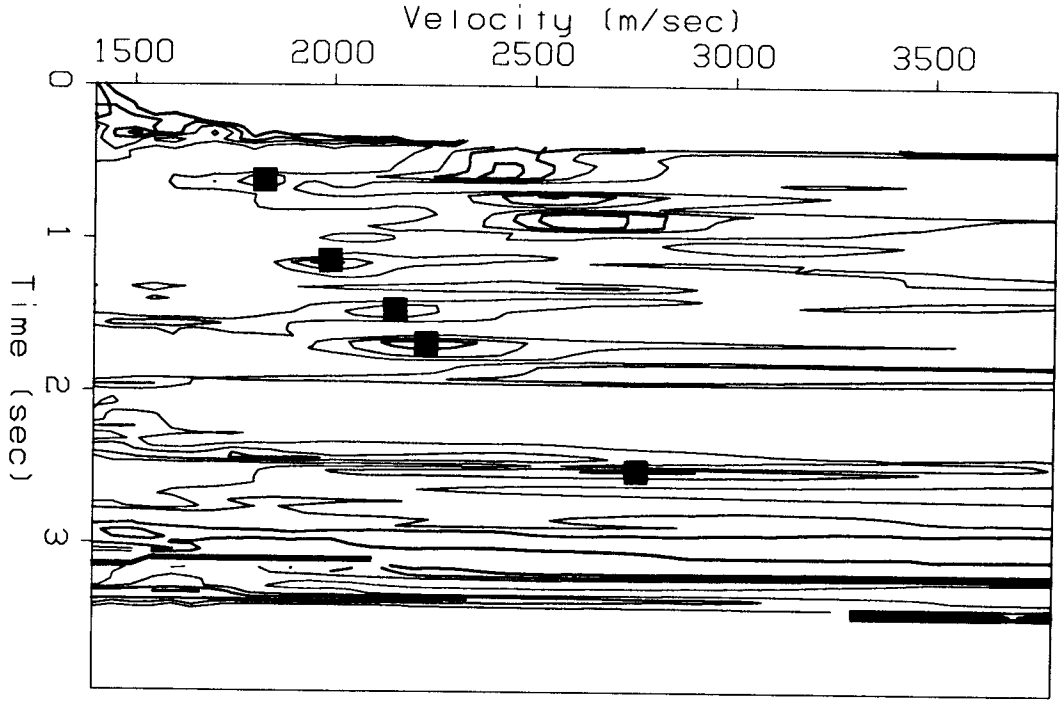

FIG. 13. Velocity analysis of a CMP gather after transformation, again at midpoint $y = 3000$ m. Squares denote converted-wave velocity picks. The velocity shown can be converted to P-wave velocity using equation (3).

Figure 13 is also a velocity analysis of a CDP gather at midpoint $y = 3000$ m, but now the data have been transformed according to equations (1) and (2). (In order to do the transformation, I had to assume that γ was already known. Since I had specified $\gamma = 1.732$ in the model, I used that same value in the transformation. For real data γ would have to be determined or guessed at beforehand.) The full unwindowed data set has been used, as it was for Figure 11. To convert the velocities in Figure 13 to S-wave or P-wave velocities, one may use equation (3) (this will give rms velocities, of course). The simplicity of conversion from v to v_s is one advantage of the transformation method: the correspondence of the velocities shown in Figures 11 and 12 to true physical velocities is not as clear.

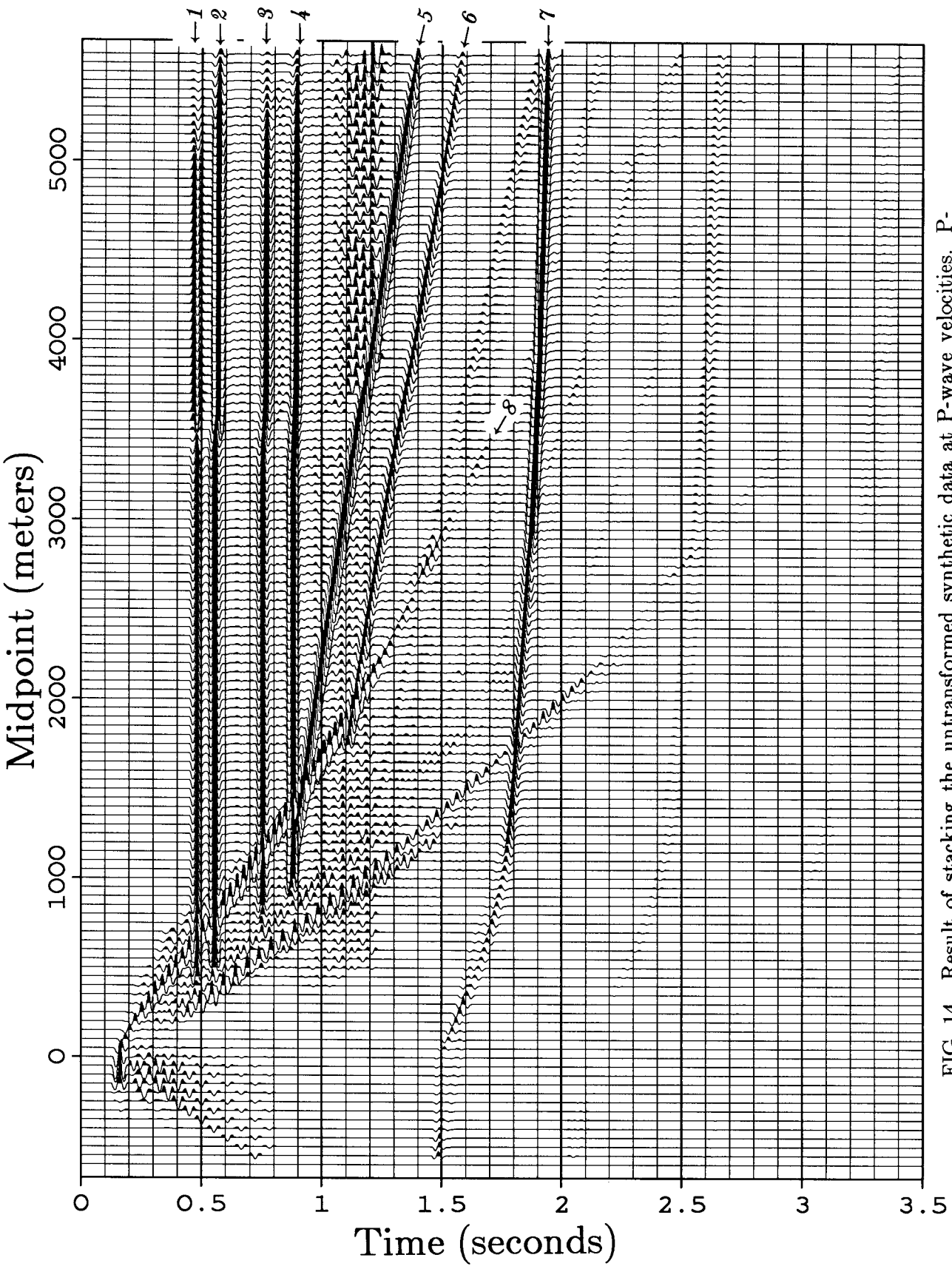

FIG. 14. Result of stacking the untransformed synthetic data at P-wave velocities. P-wave events are noted by numbered arrows; these numbers correspond to the reflector numbers in Figure 10.

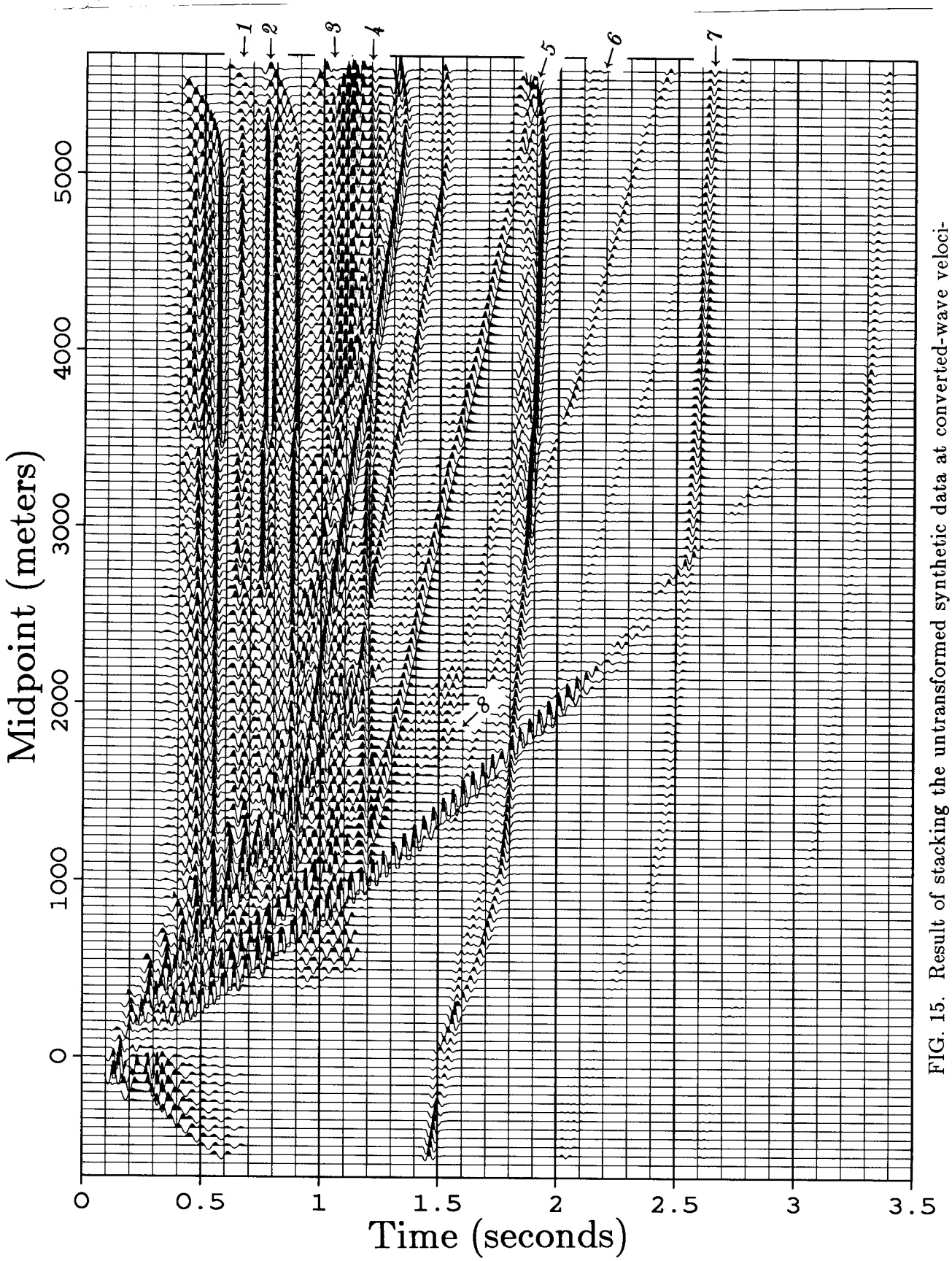

FIG. 15. Result of stacking the untransformed synthetic data at converted-wave velocities. Converted-wave events are highlighted by numbered arrows; these numbers correspond to the reflector numbers in Figure 10.

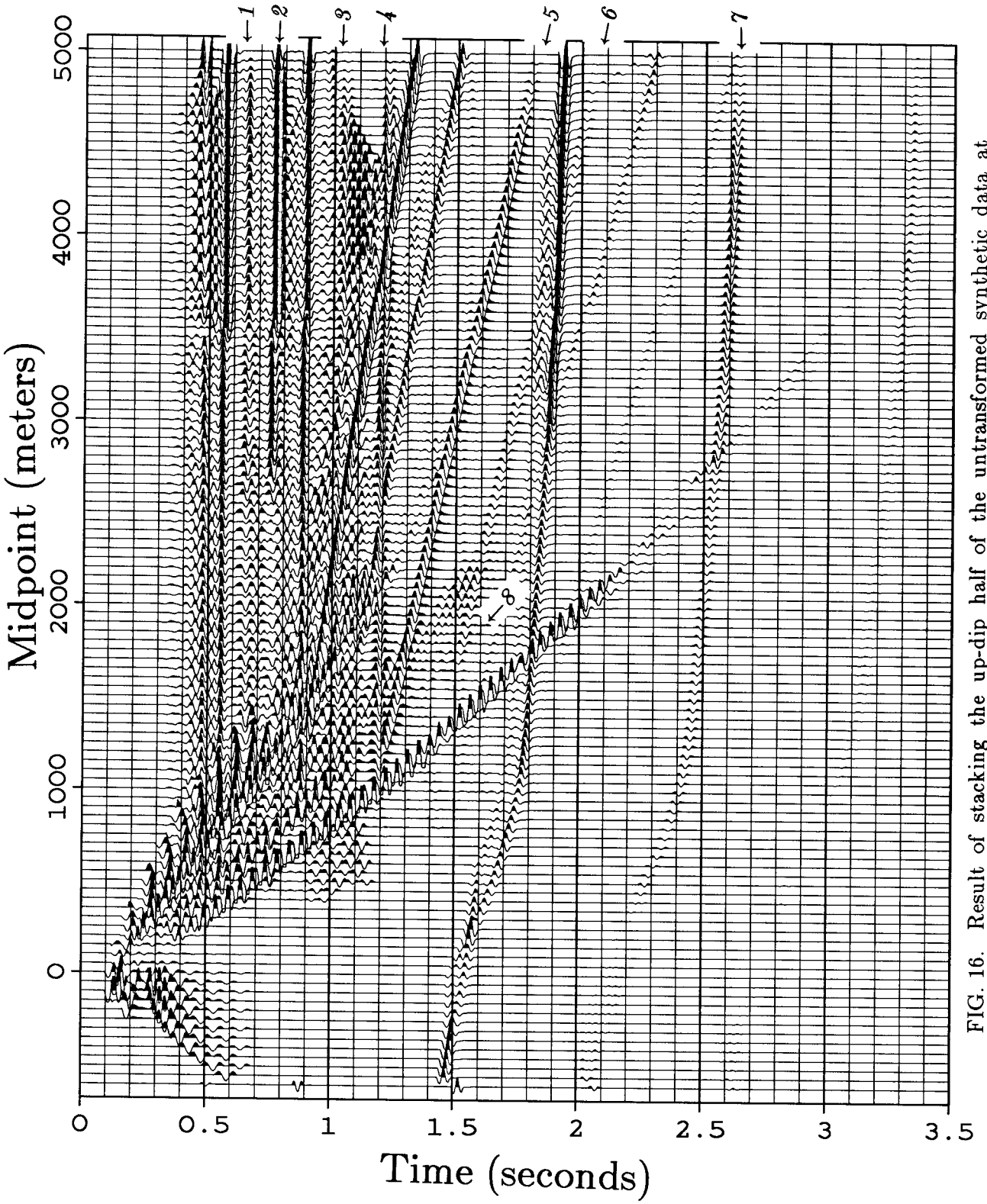

FIG. 16. Result of stacking the up-dip half of the untransformed synthetic data at converted-wave velocities. Converted-wave events are highlighted by numbered arrows; these numbers correspond to the reflector numbers in Figure 10.

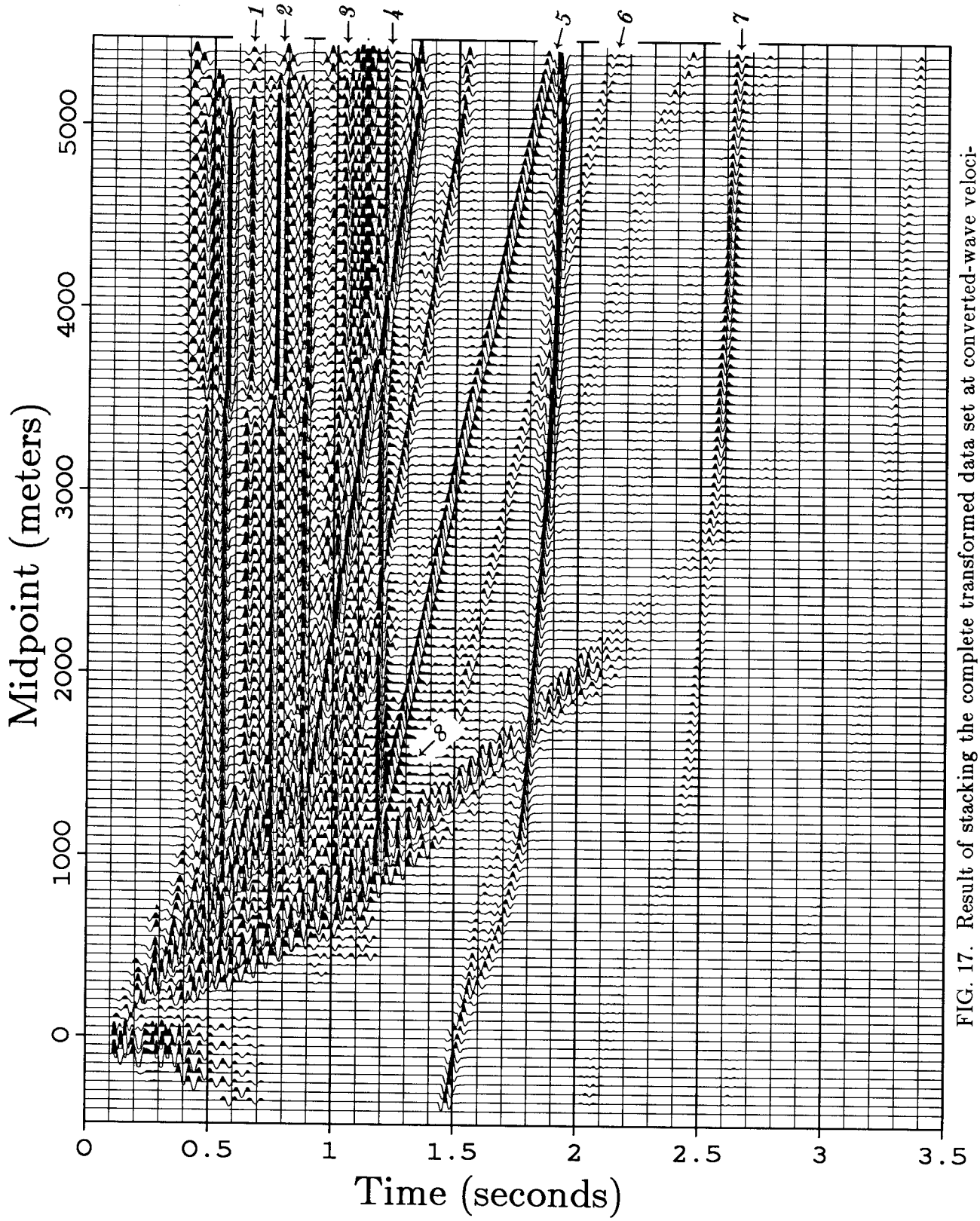

FIG. 17. Result of stacking the complete transformed data set at converted-wave velocities. Converted-wave events are highlighted by numbered arrows; these numbers correspond to the reflector numbers in Figure 10.

The next four figures, Figures 14, 15, 16, and 17, show CDP stacks of the data that was analyzed in the previous three figures. Figure 14 shows the result of stacking the untransformed split-spread data at P-wave velocities. I made this figure to provide a comparison with the converted-wave stacks in the next three figures. Figure 15 is the result of stacking the untransformed split-spread data at converted-wave velocities. Since for some converted-wave reflections two peaks appeared on the velocity analysis, presenting an ambiguity, I stacked according to the velocities found from analyzing untransformed up-dip data. That is, in order to produce Figure 15, the data that appeared in Figure 11 were stacked according to the converted-wave picks in Figure 12 (this is a simplified explanation; in order to stack the untransformed full-split-spread data, I determined a velocity function every 500 meters by analyzing the untransformed up-dip data). Figure 16 was produced simply by stacking the untransformed up-dip data according to velocity analyses based on the untransformed up-dip data. Figure 17 was produced by stacking the full split-spread transformed data set according to velocity analyses based on that very same data.

The results are reasonably favorable. There is some improvement from Figure 15 to Figure 16: the SP reflections are clearer and are not so obscured by PP reflections. The steepest-dipping reflector, number 8, is noticeably more coherent. The improvement from Figure 16 to Figure 17 is also marked. The flat reflectors, especially reflectors 1, 2 and 3, become more coherent (in fact, reflector number 3 is visible only on Figure 17). There are some tradeoffs, however; reflector number 8 almost completely disappears from Figure 17. This disappearance is due to a loss of coherence caused by the crude interpolation scheme used. Thus, there is a noticeable improvement when one uses only the up-dip data (assuming that there is a predominant dip) in the processing of SP converted-wave data; there is even more improvement when one transforms to the new coordinate system before processing. One surprise (for me) was that most of the improvements came in the images of the flat-lying reflectors; I had expected dipping reflectors to show the most improvement.

The results are gratifying, but there are some caveats. The improvement in image quality may have been because of the coordinate transformation that was applied, but there may be other causes as well. One possibility is that I may have used more accurate stacking velocities when I stacked the transformed data. If I were to pick the wrong stacking velocities for the untransformed data, it would not be surprising if I got poor results. One also must be aware of the effects of different plotting parameters. For instance, reflector 5 in Figure 17 looks stronger than the same reflector in Figure 16. This improvement is not because of the coordinate transformation but because of

differences in plotting parameters (all reflectors in Figure 17 appear stronger). Thus I have paid attention to improvements in reflector coherence rather than in reflector strength.

It should be noted that there is room for further improvement, especially in interpolation. Recall that reflector 8 was almost destroyed in Figure 17, probably because of interpolation problems. Clearly it is important that the spacing between shots and geophones not be too great.

CONCLUSIONS

In this paper it has been shown how a simple transformation of midpoint and offset coordinates can be used to make converted-wave data look approximately like conventional seismic data. This transformation has been shown to work even when $v_s = v_s(z)$, as long as γ is constant. Encouraging results were obtained when the transformation was tested on some synthetic data. It was seen that the success of the method depends to some extent on how well interpolation can be performed.

There are a couple of potential problems with the transformation method that has been presented here. One problem is that this method requires that γ be known, and that it be constant over the entire section. Real data might not satisfy either of these conditions. Another possible difficulty is that S waves typically show anisotropy more strongly than do P waves, and this anisotropy can be expected to have a certain effect on the kinematics of converted waves; that effect has not been examined here.

Despite the problems, though, there are advantages to this method (a version of it has been used for several years by Soviet geophysicists), and it clearly warrants testing on real data. I am open to any offers of two-component data that can be used to further test this method.

ACKNOWLEDGMENTS

Many of the ideas in this paper were developed during my 9-month stay at the Gubkin Institute of Petrochemical and Gas Production in Moscow. This stay was made possible by the International Research and Exchange Board, which oversees, among other programs, an exchange of graduate students and young faculty members between the US and the USSR. I should also mention Boris Zavalishin of the Gubkin Institute, who also helped make my stay possible, and Dr. G.V. Matveenko of VNII Geofizika, who provided the synthetic data set used in this paper. I would especially like to thank Drs. Puzyrev and Nefedkina of the Institute of Geology and Geophysics, in Novosibirsk, who

were kind enough to discuss their ideas with me during my visit there. Fannie Toldi helped edit this paper (any remaining mistakes are mine). And of course I thank Jon Claerbout, who talked me into visiting the USSR, and the sponsors of the Stanford Exploration Project, whose contributions provided the facilities for me to test my ideas when I returned to the US.

REFERENCES

Hale, I.D., 1983, Dip-moveout by Fourier transform: Stanford University, Ph.D. thesis (also published as SEP-36).

Nefedkina, T.V., 1980, Detection of transformed reflected PS waves by the CDP method with nonsymmetrical sampling: Soviet Geology and Geophysics 21, no. 3, pp. 93-101 (in English).

Nefedkina, T.V., Kondakova, G.P., and Oleinik, L.V., 1980, Digital processing of transformed reflected waves: Soviet Geology and Geophysics 21, no. 4, pp. 51-59 (in English).

Puzyrev, N.N., 1975, Methods of interpreting travel-time curves of transformed reflected PS waves: in collection, Problems of the theory and interpretation of seismic waves, rotaprint of the Institute of Geology and Geophysics, Novosibirsk (in Russian; probably not available outside the USSR).

Sword, C., 1984, The method of controlled directional reception: SEP-41 (this volume).

APPENDIX

The explanation of how I derived equations (1), (2), and (3) is presented in this Appendix. We begin with the equation for the travel-time curve of a wave reflected from a point diffractor at point $(x_R\ ,\ z_0)$:

$$t = \frac{1}{v_s}\sqrt{(x_R + h)^2 + z_0^2} + \frac{1}{\gamma v_s}\sqrt{(x_R - h)^2 + z_0^2} \quad . \tag{A-1}$$

Recall that x_R is the reflector position relative to the midpoint, y, of the observation system. If we are concerned with non-converted waves (PP or SS waves), then $\gamma = 1$, and we can easily solve equation (A-1) for z_0:

$$z_0^2 = \left(1 - \frac{4h^2}{v^2 t^2}\right)\left(\frac{v^2 t^2}{4} - x_R^2\right) . \tag{A-2}$$

This equation, when plotted as a function of z_0 versus x_R (with all other variables held constant), produces an ellipse (the aplanat). This ellipse is probably familiar to those who have dealt with non-zero-offset sections. Its center of symmetry is located at $x_R = 0$.

The algebra generally becomes more difficult when we are dealing with converted waves. Now $\gamma \neq 1$, and solving (A-1) for z_0 yields

$$z_0^2 = \frac{1}{\left(1-\frac{1}{\gamma^2}\right)^2}\left[-\left(1-\frac{1}{\gamma^2}\right)\left((x_R+h)^2-\frac{1}{\gamma^2}(x_R-h)^2\right)+\right. \tag{A-3}$$

$$\left.+\left(1+\frac{1}{\gamma^2}\right)v_s^2t^2-\frac{2v_s\,t}{\gamma}\sqrt{v_s^2t^2-4x_R\,h\left(1-\frac{1}{\gamma^2}\right)}\right].$$

When plotted as a function of z_0 versus x_R, this equation produces a figure that looks somewhat like an ellipse . One of the main differences between this pseudo-ellipse and the true ellipse of (A-2) is that the pseudo-ellipse has its approximate center of symmetry (only approximate, because the pseudo-ellipse isn't quite symmetrical) not at $x_R = 0$, but slightly off to one side.

Our task is to find an ellipse that approximates this pseudo-ellipse. First, let us make a zeroth-order approximation to (A-3) by setting the square-root term in (A-3) equal to $v_s\,t$. Then we can show that for this approximation, the maximum point, and thus the center of symmetry, of our pseudo-ellipse will be located at

$$x_R = -h\cdot\frac{1-\frac{1}{\gamma}}{1+\frac{1}{\gamma}}. \tag{A-4}$$

This finding suggests that we should change to a new horizontal system of coordinates

$$x_R' \equiv x_R + h\cdot\frac{1-\frac{1}{\gamma}}{1+\frac{1}{\gamma}}. \tag{A-5}$$

In this new coordinate system, our ellipse has its approximate center of symmetry at $x_R' = 0$. (This equation presents the same transformation as that in equation (1), if we make the substitutions $x_R' = x_0 - y'$ and $x_R = x_0 - y$.) This transformation was first suggested by Puzyrev (1975).

Now we substitute x_R' for x_R in (A-3), to give us

$$z_0^2 = \frac{1}{\left(1-\frac{1}{\gamma^2}\right)^2}\left[-\left(1-\frac{1}{\gamma^2}\right)\left(x_R'^2\left(1-\frac{1}{\gamma^2}\right)+\frac{4hx_R'}{\gamma}\right)+\right. \tag{A-6}$$

$$\left.+\left(1+\frac{1}{\gamma^2}\right)v_s^2t^2-\frac{2v_s^2t^2}{\gamma}\sqrt{1-\frac{4h}{v_s^2t^2}x_R'\left(1-\frac{1}{\gamma^2}\right)+\frac{4h^2}{v_s^2t^2}\left(1-\frac{1}{\gamma}\right)^2}\right].$$

So far we have made no approximations. The "proper" substitution from x_R to x_R' was found using a very rough approximation, but the substitution itself was done accurately. Now, however, we will approximate the square-root term in (A-6) by using the

Taylor-series expansion

$$\sqrt{1+x} \approx 1 + \frac{x}{2} - \frac{x^2}{8} . \tag{A-7}$$

Notice, by the way, that this expansion is exact when either $\gamma = 1$ or $h = 0$, and that it is carried out to one term further than was equation (9) in the main text.

It can be shown, after a fair amount of algebra, that when we approximate the square-root term in (A-6) using the expansion in (A-7), we obtain

$$z_0^2 \approx \left(1 - \frac{4h^2}{\gamma v_s^2 t^2}\right)\left(\frac{v_s^2 t^2}{\left(1+\frac{1}{\gamma}\right)^2} - x_R'^2\right) . \tag{A-8}$$

This is the equation for an ellipse in x_R' and z_0.

The goal now is to find a coordinate transform that will make the ellipse in equation (A-8) look like that in equation (A-2). One convenient pair of transforms is

$$h' \equiv h \cdot \frac{2}{\sqrt{\gamma}\left(1+\frac{1}{\gamma}\right)} , \tag{A-9a}$$

$$v \equiv \frac{2v_s}{1+\frac{1}{\gamma}} . \tag{A-9b}$$

(These transforms, of course, correspond to equations (2) and (3) in the main text.) By substituting equations (A-9) into (A-8) we get

$$z_0^2 \approx \left(1 - \frac{4h'^2}{v^2 t^2}\right)\left(\frac{v^2 t^2}{4} - x_R'^2\right) , \tag{A-10}$$

which is identical in form to equation (A-2).

Thus we have obtained equations (1), (2), and (3) by finding an ellipse, in the form given in equation (A-2), that would approximately fit the pseudo-ellipse given in equation (A-3). Clearly, these transformations are not unique. Anything that changes equation (A-8) into something identical in form to (A-2) will work just as well. The transforms given in (A-9) are convenient, however, in that they require changes only in y and h rather than in t or z.